AGRICULTURAL UAV CROP SPRAYING PATH PLANNING BASED ON PSO-A* ALGORITHM

/

基于 PSO-A*算法的农业无人机作物喷洒路径规划

Lijuan Fan
Xinxiang Vocational and Technical College, Xinxiang, Henan, 453006, China.
**E-mail: fanlijuan@xxvtc.edu.cn*
Corresponding author: Fan Lijuan
DOI: https://doi.org/10.35633/inmateh-71-54

Keywords: *particle swarm optimization algorithm, A* algorithm, UAV, path planning, crop spraying operations*

ABSTRACT

Currently, drones have been gradually applied in the field of agriculture, and have been widely used in various types of agricultural aerial operations such as precision sowing, pesticide spraying, and vegetation detection. The use of agricultural UAVs for pesticide spraying has become an important task in the agricultural plant protection process. However, in the crop spraying process of agricultural UAVs, it is necessary to traverse multiple spray points and plan obstacle avoidance paths, which greatly affects the efficiency of agricultural UAV crop spraying operations. To address the above issues, traditional particle swarm optimization (PSO) algorithms have strong solving capabilities, but they are prone to falling into local optima. Therefore, this study proposes an improved PSO algorithm combined with the A algorithm, which introduces a nonlinear convergence factor balancing algorithm for global search and local development capabilities in the traditional PSO algorithm, and adopts population initialization to enhance population diversity, so that the improved PSO algorithm has stronger model solving capabilities. This study designs two scenarios for agricultural UAV crop spraying path planning: one without obstacles and one with obstacles. Experimental simulation results show that using the PSO algorithm to solve the obstacle-free problem and then using the A* algorithm to correct the path obstructed by obstacles in the obstacle scenario, the agricultural UAV crop spraying trajectory planning based on the PSO-A* algorithm is real and effective. This research can provide theoretical basis for agricultural plant protection and solve the premise of autonomous operation of UAVs.*

摘要

*目前，无人机已逐步应用于农业领域，并广泛应用于精密播种、农药喷洒、植被探测等各类农业空中作业。使用农业无人机喷洒农药已成为农业植保过程中的一项重要任务。然而，在农业无人机的作物喷洒过程中，需要穿越多个喷洒点并规划避障路径，这大大影响了农业无人机作物喷洒作业的效率。针对上述问题，传统的粒子群优化算法具有较强的求解能力，但容易陷入局部最优。因此，本研究提出了一种与 A*算法相结合的改进 PSO 算法，在传统 PSO 算法中引入了一种具有全局搜索和局部开发能力的非线性收敛因子平衡算法，并采用种群初始化来增强种群多样性，使改进的 PSO 算法具有更强的模型求解能力。本研究设计了两种农业无人机作物喷洒路径规划场景：一种是无障碍场景，另一种是有障碍场景。实验仿真结果表明，在障碍场景中，使用 PSO 算法解决无障碍问题，然后使用 A*算法校正障碍物遮挡的路径，基于 PSO-A*算法的农业无人机作物喷洒轨迹规划是真实有效的。该研究可以为农业植物保护提供理论依据，解决无人机自主运行的前提。*

INTRODUCTION

Science and technology are the primary productive forces and the key support for the high-quality development of agriculture. With the increase in agricultural scale and modernization level, traditional manual pesticide spraying can no longer meet the needs of field crops *(Aggarwal S. et al., 2021)*. In order to better meet the needs of farmers, drones have been widely used in the fields *(Al-Hourani A. et al., 2014)*. With the continuous advancement and application of drone technology, drones have become a mature tool in the fields and a new weapon for pesticide spraying *(Andreev A. S. et al., 2019)*. Compared with traditional manual spraying methods, drone pesticide spraying has the advantages of high speed, high efficiency, and large-scale operation *(Batliner M. et al., 2021)*. In terms of cost, time, and expenses, drone spraying significantly reduces labor costs, saves water, and increases pesticide utilization rate by more than 30%.

In addition to the significant improvement in efficiency, using drones for pesticide spraying can automate tasks without the need for manual intervention *(Bensafia Y. et al., 2018)*. It not only protects farmers from pesticide exposure but also prevents soil and ecosystem damage *(Eschmann H. et al., 2021)*. Using drones for spraying can reduce the labor pressure on farmers and improve the comfort and safety of their work *(Hasan S. F. et al., 2020)*. These drones are equipped with advanced navigation and sensing technologies, allowing for precise spraying of field crops *(Hassan R. et al., 2020)*. By controlling flight height, speed, and liquid dosage reasonably, the amount of pesticide used can be effectively reduced, waste can be minimized, and spraying accuracy can be improved *(Huang Y. et al., 2019)*. In the long run, it can also reduce labor costs and machinery losses, saving farmers a significant amount of expenses *(Keyvan M. et al., 2020)*.

With further technological advancements, drones will be able to respond more quickly to the pest control needs during crop growth and spray pesticides in a timely manner *(Khalilpour S. A. et al., 2020),* which helps ensure the quality and yield of agricultural products *(Li P. et al., 2018)*. Moreover, traditional pesticide spraying often leads to pesticide atomization and dispersion *(Li P. et al., 2018)*, causing air and water pollution. The application of drone pesticide spraying will further achieve and improve precise spraying, reduce pesticide usage and dispersion, and minimize environmental pollution *(Li X. et al., 2019)*. By improving agricultural productivity and reducing pesticide use, rural drone pesticide spraying can create more economic benefits for farmers and enhance agricultural comprehensive benefits *(Lv S. P. et al., 2019)*. Resolving the "agriculture, rural areas, and farmers" issues is a key focus of rural industrial revitalization. In the future, high-standard farmland construction will continue to be promoted across the country, modern technology-based farming methods will be widely adopted, and agricultural production will be mechanized and intelligent *(Ou M. et al., 2022)*. With the support of "drones +", farming will become easier and smarter, and a new form of "smart agriculture" will gradually unfold in the fields *(Peng H. et al., 2020).*

Currently, in order to adapt to the development trend of modern agriculture and efficient agriculture, the Ministry of Agriculture and Rural Affairs has actively responded to the call of the central government and accelerated the construction of high-standard farmland *(Pizarro L. A. O. et al., 2020).* It focuses on implementing the rural revitalization strategy, advancing land storage and technology storage, and making the improvement of grain production capacity a top priority. This indicates that the distribution of farmland will shift from dispersed to regular and concentrated development, and agricultural plant protection will face the demand for large-scale operations *(Ren B. et al., 2020)*. Only through modern agricultural machinery and equipment can this be effectively solved, creating broad application space for aerial plant protection represented by drones. Unmanned Aerial Helicopter (UAH) plays an important role in agricultural plant protection with its characteristics of large payload, long endurance, hovering, and vertical takeoff and landing *(Rubio J. et al., 2020)*. It will also become the development direction of new intelligent agricultural machinery and equipment.

Currently, UAH and rotary drones have been widely used in the prevention and control of pests and diseases in crops such as rice, cotton, and jujube *(Santos C. et al., 2020)*. However, there is still a long transition phase from "spraying" to "spray irrigation", and automatic or autonomous flight based on flight routes is one of the effective ways to improve agricultural plant protection efficiency. In previous studies, three commonly used spraying methods in irregular operating areas for plant protection were summarized, and a reasonable scanning route planning method based on graph theory was proposed to plan rational routes from the perspectives of route selection, waypoint collection, and obstacle avoidance, enabling UAH to operate autonomously *(Talak R. et al., 2019)*. However, most of the current research is based on the ideal route planning design of a single operating area. Considering the complex conditions of flight constraints, task constraints, and obstacle constraints in actual UAH flights, it is necessary to optimize the segmentation of large-scale regular rectangular plant protection areas to ensure the efficient flight of UAH in plant protection processes and meet practical operational requirements *(Wang F. et al., 2017)*. In view of this, this paper proposes a crop protection route segmentation method based on "spraying unit modules". Firstly, the full coverage operation mode of UAH is determined *(Wang G. et al., 2021)*, and then, the minimum spraying operation unit during plant protection operations is determined as the objective function based on the flight distance of the unmanned aerial vehicle in the non-flow spraying mode *(Wang H. et al., 2021)*. The concept of minimum module segmentation is adopted to optimize the rectangular farmland. Finally, the overall planning of the plant protection operation area and the optimization design of the operation route are achieved *(Welabo A. et al., 2020)*.

With the development of smart agriculture, computer vision has achieved good results in the field of agriculture *(Xu B. et al., 2015)*. For example, *You et al. (2021)* implemented an automatic weed identification system in a pasture with broadleaf weeds *(You X. et al., 2021)*. Zeng et al. (2019) proposed a cucumber leaf pest identification system *(Zeng Y. et al., 2019) (Zeng Y. et al., 2019)*. In addition, with the maturity of deep learning (DL) technology, it has been widely used in the field of agriculture in China *(Xu J. et al., 2018).* With the increase in the number of samples, deep learning technology has become more widely used and accurate in the classification and identification of crops and pests *(Yang F. et al., 2018)*.

However, there is relatively little research on how to achieve process automation after identification. Drones are gradually transitioning from the military field to the civilian field, and their combat strategies can be introduced to the agricultural sector *(Zhang F. et al., 2014)*. Drone trajectory planning is the basis of drone combat research and the basic guarantee of drone combat effectiveness. The model considers three different methods, covering most drone flight missions *(Zhao J. et al., 2020)*. Established a target function based on flight time and flight safety factors, used fuzzy technology to assess threat levels, and applied particle swarm optimization (PSO) search strategy to drone trajectory planning *(Zhao J. et al., 2021)*. Currently, swarm intelligence optimization algorithms are relatively popular in the field of drone trajectory planning, but swarm intelligence optimization methods are prone to local optima and cannot fundamentally solve the problem. Existing two-dimensional drone trajectory planning algorithms rarely consider the influence of obstacle space on trajectories.

In summary, an improved particle swarm optimization algorithm combined with the A* algorithm is proposed for drone trajectory planning in agricultural spraying operations. The PSO algorithm introduces the K-Means clustering algorithm to initialize the population to enhance population diversity, and nonlinear convergence factor to balance global search and local development capabilities, and the PSO algorithm's position update adjustment is introduced to avoid local optimization problems. The PSO algorithm is used to plan obstacle-free crossing trajectories for multiple marked spray tasks, and then the A* algorithm is used to locally avoid obstacles in the trajectory of the obstacle path.

MATERIALS AND METHODS

The fitness function can calculate the cost of the track and compare the cost values of different tracks to determine the quality of the track. This article comprehensively balances three factors: track length, obstacle collision, and height change, and models the fitness function:

$$F = \varphi_1 f_L + \varphi_2 f_C + \varphi_3 f_H \tag{1}$$

Among them: f_H represents the cost of height change, f_C represents the cost of obstacle collision, f_L represents the cost of track length, F represents the cost of track, φ_1 φ_2 φ_3 represents the weight values of different costs, and is a constant, and its proportion is related to the tasks performed by the drone.

(1) Track length cost. The length of the drone's flight path is one of the important indicators for evaluating the quality of the flight path. Considering the limited energy supply of the drone, the shorter the flight path, the less time and energy consumption, and the more advantageous it is for the drone. Assuming the number of trajectory nodes is n, and after smoothing through interpolation, the entire trajectory consists of N nodes. (x_i, y_i, z_i) and $(x_{i+1}, y_{i+1}, z_{i+1})$ represent the three-dimensional coordinates of the i-th node and the adjacent next node, respectively. Therefore, the cost of track length can be expressed as:

$$f_L = \sum_{i=1}^{N-1} \sqrt{\left(x_{i+1} - x_i\right)^2 + \left(y_{i+1} - y_i\right)^2 + \left(z_{i+1} - z_i\right)^2} \tag{2}$$

(2) Obstacle collision cost. When the flying altitude of the drone is lower than the height of the obstacle and the distance from the center point of the obstacle is less than the radius of the obstacle, a collision occurs. In order to maintain a certain distance between track nodes and obstacles, it is necessary to calculate the collision cost of obstacles:

$$f_C = \sum_{i=1}^{T} \sum_{j=1}^{N} C_{i,j}, C_{i,j} < R_{obsi} \tag{3}$$

$$C_{i,j}=\begin{cases}\sqrt{\left(x_i-x_j\right)^2+\left(y_i-y_j\right)^2}, & z_i \geq z_j \\ 0, & z_i \geq z_j\end{cases} \quad (4)$$

Among them, N is the total number of nodes after the smooth trajectory, T is the number of obstacles, R_{obsi} is the radius of obstacle i, and $C_{i,j}$ is the distance between the i-th obstacle and the j-th trajectory node.

(3) Highly variable costs. In order to prevent collisions with mountains or other obstacles and avoid radar search, drones must raise or lower their altitude, but repeated raising and lowering may also endanger the safety of drones. Therefore, it is necessary to constrain altitude changes, and the variance of track altitude can describe the stability of flight altitude as the cost of altitude changes:

(4) Highly variable costs. In order to prevent collisions with mountains or other obstacles and avoid radar search, drones must raise or lower their altitude, but repeated raising and lowering may also endanger the safety of drones. Therefore, it is necessary to constrain altitude changes, and the variance of track altitude can describe the stability of flight altitude as the cost of altitude changes:

$$f_H=\sqrt{\frac{1}{N}\sum_{k=1}^{N}\left(z_k-\frac{1}{N}\sum_{k=1}^{N}z_k\right)^2} \quad (5)$$

In the formula: z_k is the altitude value at the k-th track node, and N is the total number of track nodes.

A* Algorithm

The A* algorithm is a heuristic search method with high search efficiency, which can solve the shortest and most effective path in a static environment. In A*, the weight of each path is the sum of two costs, namely the cost and the heuristic distance from the starting node to the current node. Starting from the starting point, it is possible to search for 8 directions, use the evaluation function to obtain the values of the extension nodes for comparison, select the minimum value as the next extension node, and cycle this process until the search is completed. Finally, the final path was obtained. Because each search uses the lowest estimated node as the next expansion node, the final cost is the lowest. The evaluation function is shown in equation (6):

$$f(n)=g(n)+h(n) \quad (6)$$

In equation (1): $h(n)$ is the estimated cost from node n to the endpoint; $g(n)$ is the actual cost from the starting node to node n; $f(n)$ is the evaluation function of node n.

The determination of the valuation function is closely related to the actual situation and will directly affect the results of the A* algorithm. Therefore, the Manhattan distance is used as a heuristic function:

$$h(n)=\left|x_d-x_n\right|+\left|y_d-y_n\right| \quad (7)$$

In equation (2): x_n is the abscissa of node n; y_d is the ordinate of the target point; x_d is the abscissa of the target point; y_n is the ordinate of node n.

The A* algorithm is a heuristic search algorithm used to evaluate each search location during path planning, the evaluation function is shown in equation (8):

$$F(n)=G(n)+H(n) \quad (8)$$

In the formula: is the estimated cost of the optimal path from the n-th node to the target node. The actual cost from the starting point to the n-th node. The search process is identified through the OPEN table and the CLOSED table. The OPEN table records the nodes to be searched, the CLOSED table records the nodes that have been searched, and the OPEN table continuously rearranges according to the evaluation function to find the best node to achieve the search process.

Improved Particle Swarm Optimization Algorithm

The basic idea of the PSO algorithm is to seek the optimal solution through information sharing and mutual reference between individuals. Firstly, each particle represents a candidate solution in the PSO, and due to the randomness of the elementary particles, random solutions can be used to initialize them.

Secondly, by using a defined fitness function to evaluate particle state, individual optimal positions and global optimal positions can be obtained through comparison. Then, each iteration, the particles will reference and update their positions and velocities, and will also dynamically update. Through repeated iterations, the optimal solution is ultimately obtained. In this article, each particle represents a trajectory. Considering trajectory planning in three-dimensional space, assuming the number of trajectory nodes is n, for the k-th particle, equation (9) represents its position vector, and equation (10) represents its velocity vector.

$$P_k = \left[\left(P^x, P^y, P^z \right)_{(k,1)}, \cdots, \left(P^x, P^y, P^z \right)_{(k,n)} \right]^T \tag{9}$$

$$V_k = \left[\left(V^x, V^y, V^z \right)_{(k,1)}, \cdots, \left(V^x, V^y, V^z \right)_{(k,n)} \right]^T \tag{10}$$

If there are S particles in the particle swarm, there must be a single optimal position for the S particles, and for the entire particle swarm, there must also be a global optimal position, as shown in equation (11):

$$\begin{cases} p_{(k,best)} = [p_{(k,1,best)}, \cdots, p_{(k,n,best)}]^T \\ p_{best}^G \in [p_{(1,best)}, \cdots, p_{(S,best)}] \end{cases} \tag{11}$$

By substituting the position of particles into the fitness function F, the trajectory quality of particles can be evaluated. The higher the trajectory quality, the smaller the fitness function value F of the corresponding particle. For particle k, if the F-value after the t-th iteration is less than the value of the previous t -1st iteration, it will be updated. Otherwise, its historical best position will still be used, as shown in equation (12). Finally, among the historical optimal positions of S particles, choose the one with the lowest F-value as the global optimal position, as shown in equation (13):

$$P_{(k,best)}(t) = \begin{cases} P_{(k,best)}(t-1); & F\left(P_{(k,best)}(t-1)\right),, F\left(P_k(t)\right) \\ P_{(k,best)}(t); & F\left(P_{(k,best)}(t-1)\right) > F\left(P_k(t)\right) \end{cases} \tag{12}$$

$$F(P_{best}^G(t)) = \min[F(P_{(1,best)}(t)), \cdots, F(P_{(s,best)}(t))] \tag{13}$$

In the next iteration, the velocity and position of each particle are updated according to equation (14) as follows:

$$\begin{cases} V_k(t+1) = w \cdot V_k(t) + c_1 \cdot r_1 \cdot \left(P_{(k,best)} - P_k(t)\right) + c_2 \cdot r_2 \cdot \left(P_{best}^G(t) - P_k(t)\right) \\ P_k(t+1) = P_k(t) + V_k(t+1) \end{cases} \tag{14}$$

In the formula, w represents the inertia weight used to inherit the velocity of particles, and is the learning factor representing the learning ability to the best state of one's own history. The learning factor represents the learning ability of the optimal individual in the group, which is any random number between 0 and 1. It is also an arbitrary random number between 0 and 1.

The inertia weight w directly affects the search ability of particles. The larger the value, the better the particle inherits the original speed, resulting in higher speed and stronger global search ability. By dynamically changing the value of inertia weight w, it is convenient to adjust the global and local search capabilities of particles at different time periods. This article adopts an exponential form of inertia weight adjustment method to improve convergence speed:

$$w = (w_{\max} - w_{\min}) \cdot \exp\left[(1-t) \cdot \alpha\right] + w_{\min} \tag{15}$$

$$t \in \left[1, 2, \cdots T_{\max}\right] \tag{16}$$

In the formula (15), w_{min} is the minimum value of w, w_{max} is the maximum value of w, T_{max} is the maximum number of iterations, t is the current number of iterations, α is used to control the decay rate of inertia weight, and is a constant coefficient.

Traditional particle swarm optimization algorithms have poor population diversity. Introducing evolutionary operators such as crossover and mutation into its algorithm can effectively improve the diversity

of the population and avoid generating local optima. The commonly used mutation operators include Gaussian mutation (GM) and Cauchy mutation (CM). Due to the large range of random numbers and low peaks in the Cauchy distribution, introducing the Cauchy mutation operator in the PSO algorithm is more advantageous for particles to quickly jump out of local extremum and increase population diversity. If x satisfies the condition given in equation (17), it will become a Cauchy distribution.

$$f(x;x_0,\gamma)=\frac{1}{\pi}[\frac{\gamma}{(x-x_0)^2+y^2}] \tag{17}$$

$$x\in(-\infty,+\infty) \tag{18}$$

where: y is the width of x_0 related to half, and x_0 is the position of the maximum value of the function. When $x=1$, $x_0=0$ and x satisfy the condition of probability density function, equation (19) is its cumulative distribution function:

$$F(x;0,1)=\frac{1}{\pi}\arctan(x)+\frac{1}{2}, \tag{19}$$

$$x\in(-\infty,+\infty) \tag{20}$$

By performing an inverse transformation on equation (19), the inverse function can be obtained, and then the random numbers generated through uniform distribution can generate random numbers that follow the Cauchy distribution:

$$\begin{cases}\frac{1}{\pi}\arctan(CM)+\frac{1}{2}=Rand\\ CM=\tan\left[\pi(Rand-\frac{1}{2})\right]\end{cases} \tag{21}$$

In the equation, $Rand$ is any real number uniformly distributed within the range of (0,1), and CM is the Cauchy mutation operator.

Similar to inertia weights, the step size of Cauchy mutation also needs to be dynamically adjusted in order to generate certain large step size disturbances in the early stages of algorithm operation, causing particles to jump out of the current position and avoid local optima. In the later stage, convergence is accelerated in smaller steps, and the update rule for each particle in each iteration is:

$$P_k^{'}=P_k+P_k\cdot CM\cdot\exp\left[(1-t)\cdot\beta\right] \tag{22}$$

$$t\in\left[1,2,\cdots,T_{\max}\right] \tag{23}$$

In the formula, $P_k^{'}$ is the position of particle k after Cauchy mutation, T_{max} is the maximum number of iterations, P_k is the position of particle k, β is the current number of iterations, is a constant coefficient, used to control the speed of variation step size.

Algorithm Steps

In summary, the implementation steps of the 3D trajectory planning algorithm for agricultural drone spraying based on PSO-A* algorithm are as follows:

Step 1: Create an agricultural drone spraying environment based on the A* algorithm, and set the starting and ending points of the drone;

Step 2: Initialize the particle position and various parameters, including the total number of particles S, maximum number of iterations, maximum speed, number of track nodes n, maximum inertia weight, total number of track nodes n, minimum inertia weight, learning factors C1, C2, etc.

Step 3: Smoothing a trajectory containing only n trajectory nodes through cubic spline data interpolation to obtain a trajectory containing n trajectory nodes, which is used to calculate the fitness values of particles in equations (9) to (14);

Step 4: Find the individual and global optimal positions of each particle;

Step 5: Update the Cauchy mutation operator CM using equation (20), and obtain the particle position for the next iteration using equation (21); Update the inertia weight w using equation (17);

Step 6: Update particle velocity V_k and position P_k according to equation (16), where if V_k and P_k cross the boundary, take the boundary value;

Step 7: Repeat steps 3 to 6 until the final flight path for agricultural drone spraying is obtained.

RESULTS

Assuming the agricultural drone spraying operation area is T (L × W, where L is the horizontal length and W is the vertical length), under the same initial conditions (environmental factors, aircraft status, payload, etc.), the PSO algorithm, A* algorithm, and PSO-A* algorithm are used to achieve complete coverage of the target spray points.

PSO Algorithm for Obstacle-Free Trajectory Planning

The simulation experiment scene is set as a 700 m × 700 m agricultural drone spraying operation area. The specific distribution of the spray points in the operation area is shown in Table 1. The particle swarm algorithm is used to solve the path planning problem for multiple spray points in obstacle-free space. In the experiment, the parameters of the particle swarm optimization algorithm are set as follows: 50 particles, maximum iterations of 200 times, and learning factors C1 and C2 both set to 1.5. When the number of spray points is 30, the convergence curve of the PSO algorithm is shown in Figure 2, and the path planning of the PSO algorithm is shown in Figure 3. From Figure 2, it can be seen that the fitness curve of 30 task points in the PSO algorithm converges, and the optimal traversal path is found in the 98th iteration of the PSO algorithm. The PSO algorithm has good convergence effect, indicating that the PSO algorithm has strong modeling and solving capabilities.

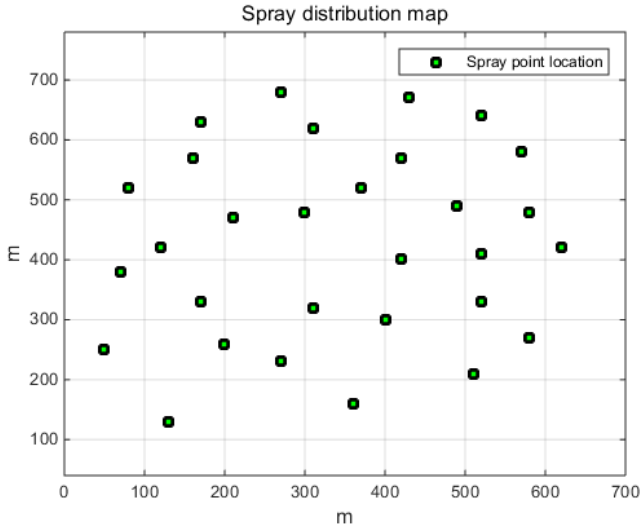

Fig. 1 - Operation area length and spraying point location coordinates (m)

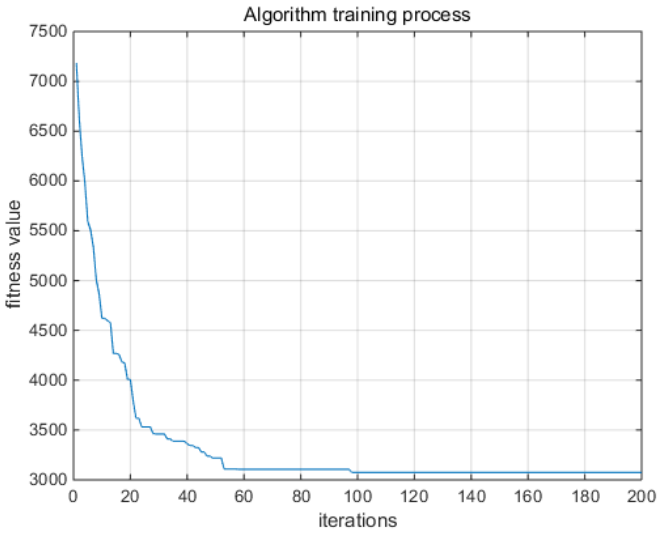

Fig. 2 - PSO algorithm convergence curve

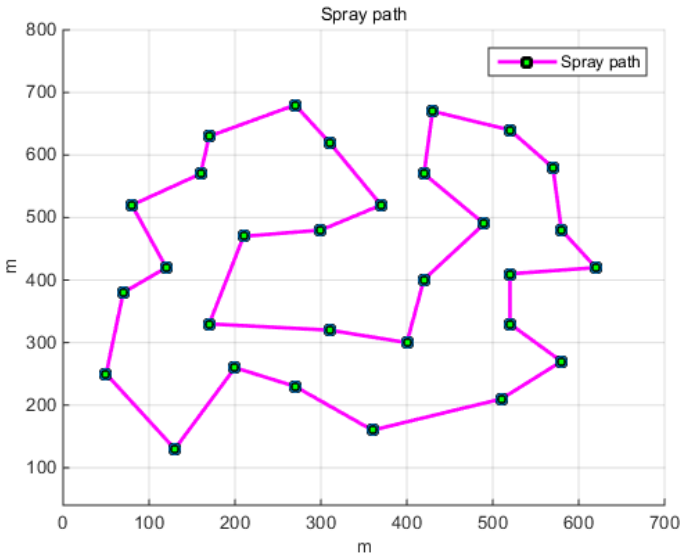

Fig. 3 - PSO algorithm track planning path

A* Algorithm Obstacle Avoidance Trajectory Planning

Obstacle avoidance trajectory planning based on A* algorithm, where the coordinates of building obstacles and spraying points are shown in Figure 4. Interactively mark obstacle areas to generate obstacle map masks. The obstacle area of the building is not accessible, and other areas are free to pass through.

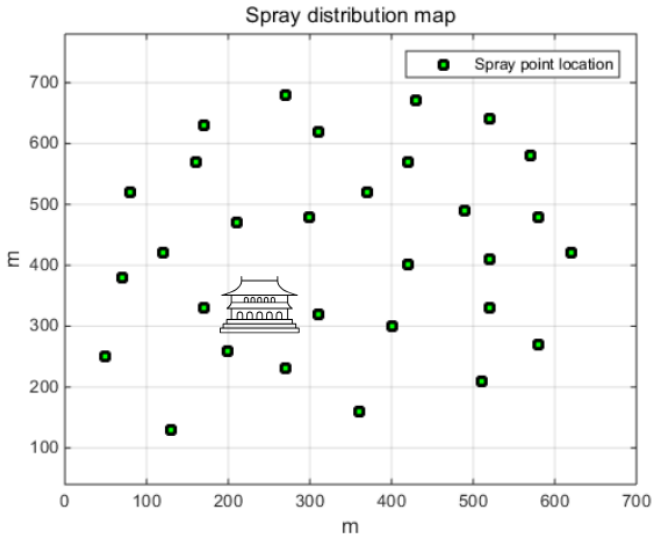

Fig. 4 - Coordinates of barrier buildings and spraying points (m)

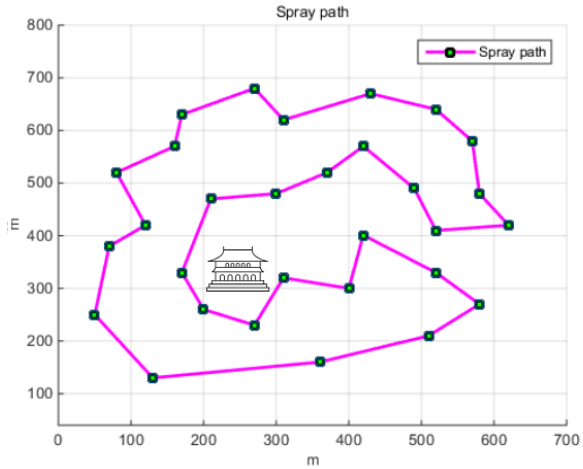

Fig. 5 - A* algorithm track planning path

Using the A* algorithm to avoid obstacles and plan the spraying trajectory of agricultural drones with obstacles at the work site. The trajectory planning effect is shown in Figure 5, and it can be seen from the figure that the A* algorithm has a good effect on obstacle avoidance trajectory planning. Taking into account the length and smoothness of the trajectory, the A* algorithm can be selected for obstacle avoidance trajectory planning.

Path Planning of Farmland Spraying Drones Based on PSO-A* Algorithm

Using PSO-A* algorithm to solve the trajectory planning problem of multiple spraying points in obstacle space. During the experiment, the parameters of the particle swarm optimization algorithm were set to 50 particle swarms, with a maximum number of iterations of 200, and learning factors C1 and C2 of 1.5. When the number of spraying points is 30, the convergence curve of the PSO-A* algorithm is shown in Figure 6, and the trajectory planning of the PSO-A* algorithm is shown in Figure 7. When agricultural drones spray in farmland areas, when obstacles are found in the planned trajectory from spraying point 16 to spraying point 9, the A* algorithm is used for obstacle avoidance secondary trajectory planning. The trajectory section starts at the coordinates of spraying point 16 and targets at the coordinates of spraying point 9 to correct this route. Figure 7 shows the A* algorithm's search for obstacle avoidance secondary correction effect trajectory, resulting in the trajectory planning results of unmanned aerial vehicles with multiple spraying points in farmland.

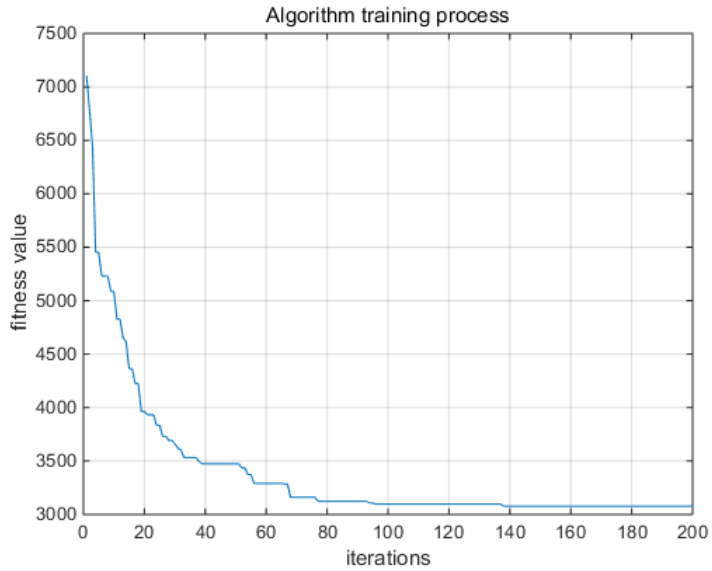

Fig. 6 - PSO-A* algorithm convergence curve

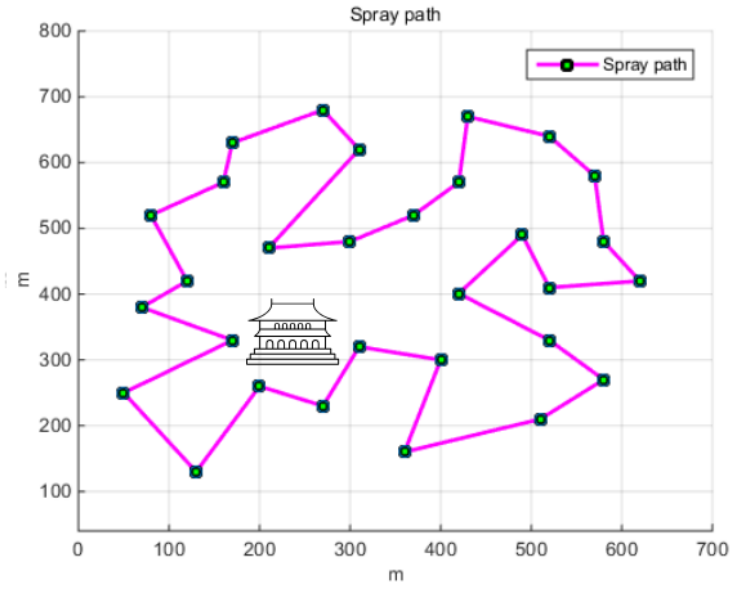

Fig. 7 - PSO-A* algorithm track planning path

CONCLUSION

This study proposed a field trajectory planning method for agricultural drones based on the PSO-A* algorithm. According to the actual requirements of agricultural drone field spraying, the multi-area operation trajectory problem was transformed into an optimization model of the particle swarm algorithm. Trajectory planning is a very complex optimization problem, and there is no absolute optimal solution in theory, only approximate optimal solutions can be obtained.

In addition to planning the flight trajectory of the drone, this study also optimized the low-altitude obstacle avoidance trajectory to better adapt to the requirements of low-altitude mission scenarios. The proposed trajectory planning algorithm for plant protection drones based on the PSO-A* algorithm can better find the approximate optimal trajectory of the plant protection drone in actual plant protection operations.

The PSO-A* algorithm has stronger capabilities in solving the trajectory planning model for drone spraying operations. The optimal traversal trajectory was found in the 98th iteration. The particle swarm algorithm has good convergence effect, indicating strong modeling and solving capabilities. In an environment with obstacles, the A* algorithm was used to avoid obstacles and plan the trajectory of agricultural drones in operational areas with obstacles. The A* algorithm has good performance in obstacle avoidance flight trajectory planning. Considering the length and smoothness of the trajectory, the A* algorithm can be used for obstacle avoidance flight trajectory planning.

In summary, the combination of the particle swarm algorithm and the A* algorithm not only improves the modeling and solving capabilities of the model, but also shortens the length of the trajectory planning. By fully considering the obstacle avoidance issues during low-altitude operations, dual trajectory correction can be performed to avoid collisions, which is beneficial to the implementation of unmanned aerial field spraying operations. This study did not consider how to determine the working task points. If machine vision and deep learning recognition processes are introduced, and the sample size is large enough, automatic extraction and classification of spray points (such as pest infested areas, weed areas, etc.) can be achieved, which can improve the autonomy of unmanned agricultural spraying operation systems and promote the development of smart agriculture.

REFERENCES

[1] Aggarwal S., Kumar N., Tanwar S. (2021). Blockchain-envisioned UAV communication using 6G networks: open issues, use cases, and future directions. *IEEE Internet of Things Journal,* Vol. 8, Issue 7, pp. 5416–5441. United States;

[2] Al-Hourani A., Kandeepan S., Lardner S. (2014). Optimal LAP altitude for maximum coverage. *IEEE Wireless Communications Letters*, Vol. 3, Issue 6, pp. 569–572. United States;

[3] Andreev A. S., Peregudova O. A. (2019). On output feedback trajectory tracking control of an omni-mobile robot. *IFAC-Papers OnLine*, Vol. 52, Issue 8, pp. 37–42. United States;

[4] Batliner M., Breitenecker F., Krner A. (2021). ARGESIM benchmark C11 'SCARA robot' with extended trajectory tracking control. *SNE Simulation Notes Europe*, Vol. 31, Issue 1, pp. 43–51. Germany;

[5] Bensafia Y., Ladaci S., Khettab K., Chemori A. (2018). Fractional order model reference adaptive control for SCARA robot trajectory tracking. *International Journal of Industrial and Systems Engineering*, Vol. 30, Issue 2, pp. 138–156. Netherlands;

[6] Eschmann H., Ebel H., Eberhard P. (2021). Trajectory tracking of an omnidirectional mobile robot using Gaussian process regression. *Automatisierungstechnik,* Vol. 69, Issue 8, pp. 656–666. Germany;

[7] Hasan S. F., Alwan H. M. (2020). Design of hybrid controller for the trajectory tracking of wheeled mobile robot with Mecanum wheels. *Journal of Mechanical Engineering Research and Developments*, Vol. 43, Issue 5, pp. 400–414. Malaysia;

[8] Hassan R., Bendary F., Elserafi K., Ghanem A., Soliman M. (2020). Comparative study methods of trajectory tracking control for robot manipulator (Dept. E). *Bulletin of the Faculty of Engineering Mansoura University*, Vol. 40, Issue 4, pp. 1–12, France;

[9] Huang Y., Mei W., Xu J., Qiu L., Zhang R. (2019). Cognitive UAV communication via joint maneuver and power control. *IEEE Transactions on Communications*, Vol. 67, Issue 11, pp. 7872–7888. United States;

[10] Keyvan M., Mohammad R. J., Abdollah H. K. (2020). A stable analytical solution method for car-like robot trajectory tracking and optimization. *IEEE/CAA Journal of Automatica Sinica*, Vol. 7, Issue 1, pp. 42–50. United States;

[11] Khalilpour S. A., Khorrambakht R., Damirchi H., Taghirad H. D., Cardou P. (2020). Tip-trajectory tracking control of a deployable cable-driven robot via output redefinition. *Multibody System Dynamics*, Vol. 16, Issue 4, pp. 1–28. Netherlands;
[12] Li P., Bao G., Fang X., Zhang L. (2018). Adaptive robust sliding mode trajectory tracking control for 6 degree-of-freedom industrial assembly robot with disturbances. *Assembly Automation*, Vol. 38, Issue 3, pp. 259–267. England;
[13] Li P., Xu J., (2018). Placement optimization for UAV-enabled wireless networks with multi-hop backhauls. *Journal of Communications and Information Networks*, Vol. 3, Issue 4, pp. 64–73. Germany;
[14] Li X., Xu J. (2019). Positioning optimization for sum-rate maximization in UAV-enabled interference channel, *IEEE Signal Processing Letters*, Vol. 26, Issue 10, pp. 1466–1470. United States;
[15] Lv S. P., Li D. H., Xian R. H. (2019). Research status of deep learning application in agriculture in China. *Computer Engineering and Applications*, Vol. 55, Issue 20, pp. 24-33. China;
[16] Ou M., Sun H., Zhang Z., Gu S. (2022). Fixed-time trajectory tracking control for nonholonomic mobile robot based on visual servoing. *Nonlinear Dynamics*, Vol. 108, Issue 1, pp. 251–263, United States;
[17] Peng H., Li F., Liu J., Ju Z. (2020). A Symplectic instantaneous optimal control for robot trajectory tracking with differential-algebraic equation models. *IEEE Transactions on Industrial Electronics*, Vol. 67, Issue 5, pp. 3819–3829. United States;
[18] Pizarro, L. A. O., Santibanez V., Garcia H. R., Chnin J. V. (2020). Sectorial fuzzy controller plus feedforward applied to the trajectory tracking of robot manipulators. *IFAC-Papers OnLine,* Vol. 53, Issue 2, pp. 9918–9923, United States;
[19] Ren B., Wang Y., Chen J. (2020). Trajectory-tracking-based adaptive neural network sliding mode controller for robot manipulators. *Journal of Computing and Information Science in Engineering*, Vol. 20, Issue 3, pp. 1–23. United States;
[20] Rubio J., Francisco P. C., García E., Juarez C. F., Lopez, G. J. (2020). Trajectory tracking of the robot end effector for the minimally invasive surgeries. *International Journal of Business Intelligence and Data Mining*, Vol. 16, Issue 1, pp. 66–88. China;
[21] Santos C., Espinosa F., Santiso E., Gualda D. (2020). Lyapunov self-triggered controller for nonlinear trajectory tracking of unicycle-type robot. *International Journal of Control, Automation and Systems,* Vol. 18, Issue 7, pp. 1829–1838. South Korea;
[22] Talak R., Karaman S., Modiano E. (2019). Optimizing information freshness in wireless networks under general interference constraints. *IEEE/ACM Transactions on Networking*, Vol. 28, Issue 1, pp. 15–28. United States;
[23] Wang F., Chao Z. Q., Huang L. B., Li H. Y., Zhang C. Q. (2017). Trajectory tracking control of robot manipulator based on RBF neural network and fuzzy sliding mode. *Cluster Computing,* Vol. 16, Issue 7, pp. 1–11. Germany;
[24] Wang G., Zhou J. (2021). Dynamic robot path planning system using neural network. *Journal of Intelligent Fuzzy Systems*, Vol. 40, Issue 2, pp. 3055–3063. Netherlands;
[25] Wang H., Li X., Jhaveri R. H., Gadekallu T. R. (2021). Sparse Bayesian learning based channel estimation in FBMC/OQAM industrial IoT networks. *Computer Communications*, Vol. 176, pp. 40–45. Netherlands.
[26] Welabo A., Tesfamariamr G. (2020). Trajectory tracking control of UR5 robot manipulator using fuzzy gain scheduling terminal sliding mode controller. *Journal of Mechatronics and Robotics*, Vol. 4, Issue 1, pp. 113–135. Japan;
[27] Xu B., Chen L. P., Tan Y. (2015). Research on the algorithm for minimum energy consumption path planning of multiple plant protection drones. *Journal of Agricultural Machinery*, 46 (11), pp. 36-42. Iran;
[28] Xu B., Chen L. P., Xu M. (2017). Algorithm for route planning of plant protection drones in multiple operation areas. *Journal of Agricultural Machinery*, Vol. 48, Issue 2, pp. 75-81. Iran;
[29] Xu J., Zeng Y., Zhang R. (2018). UAV-enabled wireless power transfer: trajectory design and energy optimization. *IEEE Transactions on Wireless Communications,* Vol. 17, no. 8, pp. 5092–5106. USA;
[30] Yang F., Xue Y. C., Li J. (2018). Path planning of traversal multi task target robots under static obstacles, *Journal of Tianjin University of Technology*, Vol. 37, no. 4, pp. 65-71. China.
[31] You X., Wang C., Huang J. (2021). Towards 6G wireless communication networks: vision, enabling technologies, and new paradigm shifts. *Science China,* Vol. 64, pp. 1–74. China;
[32] Zeng Y., Wu Q., Zhang R. (2019). Accessing from the sky: a tutorial on UAV communications for 5G and beyond, *Proceedings of the IEEE*, Vol. 107, Issue 12, pp. 2327–2375. United States;

[33] Zeng Y., Xu J., Zhang R. (2019). Energy minimization for wireless communication with rotary-wing UAV. *IEEE Transactions on Wireless Communications,* Vol. 18, Issue 4, pp. 2329–2345. United States;
[34] Zhang F., Wang L., Fu L. (2014). Recognition of cucumber leaf diseases based on support vector machine. *Journal of Shenyang Agricultural University*, Vol. 45, Issue 4, pp. 457-462. China;
[35] Zhao J., Huang J., Wang R., Peng H. R., Ji S. (2020). Investigation of the optimal parameters for the surface finish of k9 optical glass using a soft abrasive rotary flow polishing process. *Journal of Manufacturing Processes*, Vol. 49, pp. 26–34. United States;
[36] Zhao J., Huang J., Xiang Y. (2021). Effect of a protective coating on the surface integrity of a microchannel produced by microultrasonic machining. *Journal of Manufacturing Processes*, Vol. 61, pp. 280–295. United States;